

Genomic characteristics and clinical significance of CD56+ Circulating Tumor Cells in Small Cell Lung Cancer

4 C. RICORDEL^{*1,2}, L. CHAILLOT^{*1}, E. I. VLACHAVAS^{*3,4}, M. LOGOTHETI³, A.
 5 JOUANNIC¹, T. DESVALLEES^{5,6}, G. LECUYER¹, M. AUBRY¹, G. KONTOGIANNI⁷, C.
 6 MASTROKALOU³, F. JOUAN¹, U. JARRY^{5,6}, R. CORRE², Y. LE GUEN², T.
 7 GUILLAUMEUX^{1,5}, H. LENA^{1,2}, A. CHATZIOANNOU^{3,7}, R. PEDEUX^{1,5}

8

⁹ ¹ Univ Rennes 1, INSERM, OSS (Oncogenesis Stress Signaling), UMR_S 1242, CLCC
10 Eugene Marquis, F-35000, Rennes, France

11 ² Service de Pneumologie, CHU Rennes, Rennes, France

12 ³ e-NIOS PC, Kallithea-Athens, Greece

⁴ Division of Molecular Genome Analysis (B050), German Cancer Research Center (DKFZ),
Im Neuenheimer Feld 280, 69120 Heidelberg, Germany.

⁵ Univ Rennes, CNRS, INSERM, BIOSIT UAR 3480, US_S 018, Oncotrial, F-35000 Rennes,
France

17 ⁶Biotrial Pharmacology, Unité De Pharmacologie Préclinique, Rennes, France.

⁷ Centre of Systems Biology, Biomedical Research Foundation of the Academy of Athens, 4 Soranou Ephessiou Street, 11527, Athens, Greece.

20

²¹* These authors contributed equally to this work.

22

23

24 Corresponding author:
25 Dr Charles Ricordel
26 Service de Pneumologie, Hôpital Pontchaillou
27 2 Rue Henri Le Guilloux
28 35033 RENNES
29 France
30 Phone: +33 (0)2 99 28 37 38
31 Fax: +33 (0)2 99 28 24 80
32 Mail: charles.ricordel@chu-rennes.fr
33 ORCID ID: 0000-0001-6160-2732
34 Twitter handle: @C_Ricordel
35

36 Co-corresponding author :
37 Mr Rémy Pedeux
38 Université Rennes 1
39 CLCC Eugène Marquis, INSERM U1242-COSS
40 Rue Bataille Flandres Dunkerque
41 35042 RENNES, FRANCE
42 Tel : 33 (0)2 23 23 47 02
43 E-mail : remy.pedeux@univ-rennes1.fr
44 ORCID ID: 0000-0002-2553-7934
45

46 **Conflict of interest statement:**

47 CR declare personal and institutional financial interest as invited speaker for Takeda,
48 Astrazeneca, as advisory role for BMS, MSD and Takeda; LC declare no conflict of interest;
49 EIV declare no conflict of interest; ML declare no conflict of interest; AJ declare no conflict
50 of interest; TD declare no conflict of interest; GL declare no conflict of interest; MA declare
51 no conflict of interest; GK declare no conflict of interest; CM declare no conflict of interest;
52 FJ declare no conflict of interest; UJ declare no conflict of interest; RC personal interest as
53 invited speaker for BMS, as consulting or advisory role for Takeda, Lilly, Sanofi and
54 Astrazeneca; YLG declare no conflict of interest; TG declare personal and institutional
55 financial interest as member of the board of directors of Kineta; HL declare personal
56 financial interest as honoraria recipient for BMS, Astrazeneca, MSD, Pfizer, Sandoz, as
57 consulting or advisory role for Astrazeneca, Pfizer, Sanofi, Daiichi Sankyo/Lilly, Novartis
58 and Roche; AC declare personal and institutional financial interest as CEO of e-NIOS
59 Applications PC; RP declare no conflict of interest; CTC-CPC study was initially funded by
60 the JOTGO 2015 research grant with CR as a recipient.
61

62 **Sources of support:** Région Bretagne, La Ligue Contre le Cancer (Grand Ouest),
63 Association pour la Recherche sur le Cancer (ARC), ANR through the Labcom Oncotrial
64 projet 2014–2019 (Université de Rennes 1 – UAR Biosit – BIOTRIAL, Rennes, France) and
65 JOTGO 2015 grant from Roche® company.

66

Abstract

67 **Introduction:** Circulating Tumor Cells (CTC) have been studied in various solid tumors but
68 clinical utility of CTC in Small Cell Lung Cancer (SCLC) remains unclear. The aim of the
69 CTC-CPC study was to develop an EpCAM-independent CTC isolation method allowing
70 isolation of a broader range of living CTC from SCLC and decipher their genomic and
71 biological characteristics.

72 **Patients and methods:** CTC-CPC is a monocentric prospective non-interventional study
73 including treatment-naïve newly diagnosed SCLC. CD56+CTC were isolated from whole
74 blood samples, at diagnosis and relapse after first-line treatment and submitted to Whole-
75 exome-sequencing (WES).

76 **Results:** Phenotypic study confirms tumor lineage and tumorigenic properties of isolated cells
77 for the 4 patients analyzed with WES. WES of CD56+CTC and matched tumor biopsy reveal
78 genomic alteration frequently impaired in SCLC. At diagnosis CD56+CTC were
79 characterized by a high mutation load, a distinct mutational profile and a unique genomic,
80 compared to match tumors biopsies. In addition to classical pathways altered in SCLC, we
81 found new biological processes specifically affected in CD56+CTC at diagnosis. High
82 numeration of CD56+CTC ($>7/\text{ml}$) at diagnosis was associated with ES-SCLC. Comparing
83 CD56+CTC isolated at diagnosis and relapse, we identify differentially altered oncogenic
84 pathways (e.g. DLL3 or MAPK pathway).

85 **Conclusions:** We report a versatile method of CD56+CTC detection in SCLC. Numeration of
86 CD56+CTC at diagnosis is correlated with disease extension. Isolated CD56+CTC are
87 tumorigenic and a distinct mutational profile. We report a minimal gene set as a unique
88 signature of CD56+CTC and identify new affected biological pathways enriched in EpCAM-
89 independent isolated CTC in SCLC.

90

91 **Keywords:** circulating tumor cells; small cell lung cancer; CD56 marker; cancer genomics

92

93 **Introduction**

94

95 Lung cancer is the leading cause of cancer-related death worldwide, accounting for 1.6
96 million deaths per year (1). Small cell lung cancer (SCLC) is an aggressive subset of lung
97 cancer, representing 10 to 15% of lung cancers and characterized by rapid-onset symptoms
98 due to high tumor growth rate (2). At diagnosis, most patients present an extensive stage
99 disease (ES-SCLC) for whom the recommended treatment has been for the last decades a
100 palliative platinum-based chemotherapy regimen. Even if recently, the combination of
101 chemotherapy with immune checkpoint inhibitors showed substantial outcomes improvement
102 in two phase III trials (3,4), the prognosis remains poor with a median overall survival of
103 about one year. For patients diagnosed with limited stage disease (LS-SCLC), concomitant
104 chemo-radiotherapy is the recommended treatment option showing a median overall survival
105 of over 20 months (5).

106

107 SCLC shows a high propensity for metastatic spreading and therefore generates a higher
108 number of circulating tumor cells (CTC) compared to other tumor types (6). Recent studies
109 have demonstrated that CTC isolated from patients diagnosed with SCLC can be deeply
110 characterized at the genomic level and could have a potential prognostic significance (7–9).
111 An in-depth analysis of single-cell CTC copy number variation (CNV) by whole-genome
112 sequencing in a cohort of 31 SCLC patients was used to create a CNV classifier that could
113 reliably predict chemosensitivity (10). However, these genomic analyses, especially on single
114 cell CTC are not sustainable in routine clinical practice. Moreover, it should be noted that in
115 most studies, CTC isolation was based on the expression of epithelial markers (EpCAM). It is
116 well documented that tumor cells migrating through the bloodstream undergo epithelio-
117 mesenchymal transition (EMT), characterized by the loss of expression of epithelial markers

118 expression (11,12). Coherently, studies using a EpCAM-independent isolation method show a
119 higher detection rate of CTC (13). A recent immunofluorescence study on a large cohort of
120 108 SCLC patients demonstrate that EpCAM-based methodology (Cellsearch®) was unable
121 to detect CD56+ and/or TTF1+-CTC in more than 20% of patients (14). These results suggest
122 that CTC isolation method relying on EpCAM markers does not circumvent the issue of EMT
123 of CTC in SCLC. Consequently, there is a clear unmet need for comprehensive genomic
124 studies performed on CTC isolated independently of EpCAM to achieve a better
125 understanding of the biology of SCLC. To explore such an avenue of research, we select the
126 CD56 marker, frequently express at surface of the membrane of SCLC cells, as it will allow
127 the isolation of living CTC from the blood of SCLC patients.

128

129 Here, we describe a versatile and easy-to-use workflow for the detection, count and isolation
130 of CD56+CTC from whole blood samples in a prospective cohort of 33 newly diagnosed
131 patients with SCLC at our institution. Phenotypic analysis of isolated cells confirmed their
132 tumor lineage. Notably, generation of CTC-Derived Xenografts (CDX) in
133 immunocompromised mice support the tumorigenic properties of CD56+CTC. Our findings
134 indicate that while there are genes commonly altered in biopsies and CD56+CTC samples,
135 there is noticeable mutational diversity in the liquid biopsies, highlighting a putative distinct
136 molecular signature. Finally, CD56+CTC count at diagnosis was associated with the stage of
137 the disease.

138 **Materials and methods**

139 *Patient and samples*

140 We conducted a prospective non-interventional study in our institution (Rennes University
141 Hospital), including only patients with a histologically or cytologically confirmed
142 chemotherapy-naïve SCLC and eligible to a systemic treatment, starting from April 2016. The
143 data lock was planned in December 2021 for all patients that achieve a minimal follow-up of
144 at least 6 months. The recruitment is still active beyond this date. Any active neoplasia other
145 than SCLC or known HIV, HCV or HBV infection, were considered as exclusion criterion.
146 CD56+CTC were numerated and isolated from a whole blood sample, before the first
147 administration of any cytotoxic agent and when disease relapsed (Fig 1A). Paired tumor tissue
148 samples were obtained for four patients in order to compare CD56+CTC and biopsies
149 genomic characteristics. LS-SCLC was defined as disease confined to one hemi-thorax and
150 that could be safely encompassed in a single radiation field, otherwise patients were
151 considered ES-SCLC. The International Association for the Study of Lung Cancer (IASCL)
152 eighth edition of the TNM Classification for small cell lung cancer was used to stage patient's
153 SCLC (15). Chemosensitive status was defined as patient without progressive disease within 3
154 months after the first-line of treatment, as opposed to chemorefractory status. Progression-free
155 survival (PFS) was defined as the time from the start of chemotherapy until disease
156 progression or death from any cause and assessed using RECIST version 1.1. Overall survival
157 (OS) was defined as the time from the start of chemotherapy until death from any cause.
158 Patients who had not progressed at the time of the statistical analysis or who were lost to
159 follow-up before progression or death were censored at their last evaluation. This study was
160 conducted in accordance with the Declaration of Helsinki and was approved by Rennes
161 University hospital ethic committee (n° 15.120). All participants provided informed consent,
162 according French national regulation for non-interventional studies.

163

164 *Workflow Isolation of CD56+ CTC from whole blood*

165 The first step consists in a CTC enrichment from whole blood sample by immunomagnetic
166 negative selection using the EasySep™ Direct Human CTC Enrichment Kit (StemCell
167 Technologies®, Vancouver, Canada) according to manufacturer instruction. Because we
168 expected to isolate a very small number of cells and to accurately sort the CTCs, the
169 remaining cells were mixed with 1×10^5 PBMCs (peripheral blood mononuclear cells). Cell
170 suspension was washed in PBS 2% BSA and incubated with saturating concentrations of
171 fluorescent-labelled antibodies against human CD56, CD45 and Cd235a (Miltenyi, Bergisch
172 Gladbach, Germany) for 15 min at 4°C. Cells were then washed with PBS 2%-BSA and
173 analyzed and sorted by flow cytometry using a FACS Aria II (Becton Dickinson, Franklin
174 Lakes, NJ). The population of interest was gated according to its CD56/CD45 criteria to avoid
175 NK lymphocytes contamination (exclusion of CD56+/CD45+ cells). Cells CD56+/CD45-
176 were sorted, centrifuged, and immediately freeze at -80°C. CD45+ PBMC were used as a
177 negative control. Data were analyzed with FlowJo™ Software (Ashland, OR: Becton,
178 Dickinson and Company).

179

180 *Pathway analysis and comparison of genomic mutational patterns between biopsy and paired*
181 *CD56+ CTC*

182 Detailed methods for PBMC isolation, extraction of DNA, whole exome sequencing and
183 variant annotation workflow can be found in the supplemental data. . Complete analysis was
184 performed utilising various state-of-the-art tools. Unless stated otherwise, all bioinformatics
185 analyses were performed using shell interface command line, on a Linux-based 64GB RAM/
186 12 processor cluster server (Ubuntu 18.04). Initially, to unravel the common mutational
187 patterns between CTCs and matched biopsies, a simple Venn diagram/overlap analysis was

188 performed for each patient separately at the variant level (based on SNVs & INDELS) and at
189 the gene level. The final variants that were common in the remaining variant lists of CTC and
190 paired biopsy samples for each patient, were imported to the BioInfoMiner platform
191 (<https://bioinfominer.com>) for the functional interrogation of the perturbed pathways in the
192 CTC and biopsy samples utilizing different hierarchical and ontological vocabularies (Gene
193 Ontology & Reactome Pathways) (16). Additionally, in order to investigate the mutational
194 relatedness of CTC and biopsy samples, based on their mutational profiles in the six base
195 substitution catalogues, the R package MutationalPatterns (v 1.10.0) was used (17). Finally,
196 semantic similarity (GO functional similarity) based on the aforementioned pathway
197 enrichment analysis was performed between CTC and biopsy samples for each patient, to
198 identify any common molecular mechanisms.

199

200 *Derivation of an informative gene signature of CD56+CTC samples*

201 For the derivation of a minimal gene set, expanding the molecular profile of the circulating
202 tumor cell samples in the SCLC patients, we applied a data mining approach based on the
203 aforementioned results of the WES computational analysis (see supplemental material and
204 methods for details).

205

206 *In vivo xenograft experiments*

207 NSG (*NOD.Cg-Prkdcscid Il2rgtm1Wjl/SzJ*) mice were purchased from Charles River
208 Laboratories (Wilmington, MA). Mice were subcutaneously injected with a cell suspension
209 (obtained after the first step of circulating tumor cell isolation) on the left flank with Matrigel
210 (v/v) (Corning, Corning NY), as previously described (9). Tumor size was monitored using
211 calliper twice per week. All animal procedures met the European Community Directive
212 guidelines (Agreement B35-238-40 Biosit Rennes, France) and were approved by the local

213 ethics committee (Agreement APAFIS # 7163; CEEA - 007 regional ethics committee of Brittany;
214 France), ensuring the breeding and the daily monitoring of the animals in the best conditions
215 of well-being according to the law and the rule of 3R (Reduce-Refine-Replace). All
216 experiments were performed in accordance with relevant guidelines and regulations. After
217 tumor growth mice were euthanized (cervical dislocation) when tumors reached 1000 mm³
218 and tumors were harvested and cut in two pieces (one used for cell culture and the other for
219 formalin-fixation). All experiments on live animals are reported here in accordance with
220 ARRIVE guidelines. Refer to supplemental material & methods for RNAseq analysis and
221 identification of SCLC patient subtype.

222 Statistical analysis

223 Demographic and descriptive data are given as the median with the range. Categorical
224 variables were compared with the Fisher exact test or the Pearson X² test, and quantitative
225 variables were compared with the Mann-Whitney U test when appropriate. Two-tailed P-
226 values were reported, with P < 0.05 considered as statistically significant. The Kaplan-Meier
227 method with log-rank test was used to perform survival analysis. Finally, binomial logistic
228 regression model was built with the CD56⁺CTC count (≥ 7 CD56+CTC or ≤ 7 CD56+CTC/ml
229 of blood) as the dependent variable. The pre-specified cut-off of 7 CD56+CTC/ml was
230 chosen, based on study investigating prognosis of CTC in SCLC which shows that more than
231 50 CTC/7.5ml (equivalent to 6.6 CTC/ml) correlate with survival (6). GraphPad Prism for
232 Windows software (version 5.03; Graph Pad Software Inc, San Diego, CA) was used for the
233 statistical and survival analyses.

234 **Results**

235 *CD56+CTC isolated from whole blood samples are tumorigenic*

236 To isolate CD56+CTC from SCLC patients, we have set up a two steps protocol. First,
237 hematopoietic cells and platelets were depleted and then CD56+CTC were isolated by cell
238 sorting, using CD56 as a positive selection marker and CD45 as a negative selection marker
239 to avoid NK cells contamination (Fig 1B). Based on the technical validation of the isolation
240 method (Supplementary Fig. S2A and S2B), we processed all the samples immediately after
241 collection. A representative example of flow cytometry gating strategy used for cell sorting is
242 shown in Figure 1B (right panel). In order to establish the tumorigenic proprieties of
243 CD56+CTC, we performed CDX generation through implantation of isolated CD56+CTC on
244 the flank of nude mice, according to previous published methodology (9). Out of five
245 attempts, CD56+CTC from two patients generated tumors in mice (Figure 1C). Subsequent
246 immunohistochemistry analysis on these CDX tumors show positivity for commonly used
247 markers for SCLC diagnosis: CD56, synaptophysin and chromogranin A, demonstrating the
248 stability of the patient's neuroendocrine tumor lineage (Fig. 1D). Moreover, *in vitro* CTC-
249 derived cell lines were obtained from two patient's samples and amplified in culture (Fig.
250 1D). Consistently with the recent classification of SCLC, CDX model derived from patient 30
251 was successfully classified with an ASCL1 transcriptomic profile (Fig. 1E). Altogether, these
252 results confirmed the tumorigenic properties of CD56+CTC isolated from whole blood
253 samples of patients with a treatment-naïve SCLC.

254

255 *CD56+CTC share common genomic alterations with SCLC tissue biopsies but display a*
256 *distinct mutational signature*

257 To further characterize CD56+CTC at the genomic level, we submitted the CTC samples,
258 matched PBMC and tumor biopsies to whole-exome-sequencing for four patients in our
259 cohort. The average sequencing coverage (up to 135X and with a minimum depth of 20X)

260 was 0.70, 0.87 and 0.88 for CTC, biopsy and PBMC respectively (Table 1). Many genes
261 commonly found to be altered according to large scale genomic studies of small cell lung
262 cancer (18), were also detected in our genomic analysis (Fig. 2A). Alterations in *TP53* or
263 *RBI*, the two most consistently altered genes in SCLC, were found in CD56⁺CTC of 3
264 patients (75%). CD56+CTC from one patient didn't show any *TP53* or *RBI* mutation but
265 CNV analysis revealed a mono-allelic deletion of both genes (Fig. 2B). Moreover, our
266 analysis showed that the altered pathway commonly found in SCLC, such as NOTCH
267 signaling, were also observed in our CD56+CTC samples (Supplemental Fig. 3B). These
268 results confirmed that the genetic profiles of CD56+CTC are similar to the known genomic
269 landscape of SCLC.

270 Interestingly, the mutational load in CD56+CTC was much higher than in matched tumor
271 biopsies for all patients (Table 1). The mean mutational load in CD56+CTC and tumor
272 biopsies was 188.02 and 6.44 mutations/Mb respectively. The majority of mutations found in
273 the tissues were confirmed in CD56+CTC (except for patient 06 were only 39/103 mutations
274 where shared between samples) (Fig. 2C and supplemental material and method). C>A
275 transversion, classically associated with tobacco exposure, was the dominant mutation type in
276 the tissue biopsies (Fig. 2D). Conversely, C>T transversion (outside CpG sites) was dominant
277 in CTC, suggesting that drivers of mutagenesis might be distinct in CD56+CTC. In line with
278 this hypothesis, hierarchical clustering of samples based on their mutational patterns using
279 COSMIC mutational signatures (v2-March 2015) tended to discriminate between blood and
280 biopsy samples (Supplemental Fig.3A). Even if CTC and biopsy samples showed high
281 similarities with multiple signatures, biopsies showed a higher correlation with signature 4
282 (related to tobacco mutagens), 24 & 29 (transcriptional strand bias for C>A mutations);
283 whereas, CD56+CTC were significantly associated with signature 15 (defective DNA

284 mismatch repair) with signatures 19 & 30 (etiology unknown), supporting the idea of distinct
285 “circulating” drivers of mutagenesis in CD56+CTC.
286 To explore altered signaling pathways in CD56+CTC, we exploited BioInfoMiner (BIM)
287 web platform which implements robust statistical and network analysis for functional
288 enrichment investigation in order to highlight the most important biological mechanisms.
289 Thus, we identified a genomic signature comprised of 75 hub genes for the CD56+CTC at the
290 time of diagnosis (Fig.2E). In order to capture holistically the perturbed biological
291 components that are related to SCLC pathophysiology and progression, we utilized one of the
292 most comprehensive biomedical vocabularies REACTOME pathway analysis. Subsequent
293 functional enrichment analysis of the compact gene set revealed altered biological
294 mechanisms either directly or indirectly associated with lung cancer progression (related to
295 neural cell adhesion, extracellular matrix organization, hypoxia or immune response)
296 (Fig.2F). This analysis also stressed the importance of understudied processes in SCLC:
297 sumoylation and transcriptional regulation by AP-2 and RUNX2. Subsequently, three
298 genomic databases of SCLC (Cancer Gene Census, Intogen driver genes and
299 MycancerGenome) were analyzed with BIM leading to the identification of 22, 17 and 9 hub
300 genes respectively (Supplemental Table 1). Interestingly, 23 of the 75 hub genes from
301 CD56+CTC, such as *ERBB2*, *TP53*, *CREBBP* and *NF1*, were found enriched in at least 1 of
302 the 3 queried databases, illustrating the high affinity of the liquid biopsies to recapitulate the
303 molecular genomic landscape of small cell lung cancer. The REACTOME pathway analysis
304 of the 23 hub genes further confirmed that the altered biological mechanisms found in
305 CD56+CTCs correspond to those found in SCLC, with the addition of the p53 signaling
306 pathways (Supplemental Fig.3D).

307 Altogether, these observations support the hypothesis that CD56+CTC can reliably
308 recapitulate the mutational status of treatment-naive SCLC tumors and may represent a
309 comprehensive way of capturing the whole mutational picture of SCLC.

310

311 Cohort demographics

312 From April 2016 to April 2021, 46 patients were eligible for inclusion in the study. Seven
313 patients met the exclusion criteria and 39 patients had CD56+CTC isolation from blood
314 samples. For five patients, isolated CD56⁺CTC were used for *in vivo/ex vivo* culture and one
315 patient withdrew consent. Finally, the number of CD56+CTC at diagnosis was available for
316 33 patients who were therefore included in the statistical analysis (Supplementary Fig.4). The
317 demographic and descriptive statistics of the cohort are presented in Table 2. Patients were
318 predominantly male (69.7%), active smoker (69.7%) and had mainly an extensive-stage
319 disease at diagnosis (66.7%). Of note, a large proportion of the patients progressed within 3
320 months after the end of the first-line of chemotherapy and was considered chemorefractory
321 (45.5%). Based on the pre-specified cut-off of 7 CD56+CTC/ml, two groups of patients were
322 compared. The two groups were well balanced with respect with age, sex, smoking exposure,
323 chemosensitivity or median follow-up (Table 2). However, the group with more than 7
324 CD56+CTC/ml at diagnosis was enriched in patients with ES-SCLC (85.7% vs 52.7%),
325 without reaching statistical significance (Fisher's exact test; p= 0.067). Remarkably, the five
326 patients without any metastatic localization at diagnosis show a low CD56+CTC count (mean:
327 3.23±3.30 cells/ml). Two patients show no detectable CD56+CTC in blood samples: one had
328 LS-SCLC and the other one had a low thoracic tumor burden associated with multiple
329 cerebral and medullary metastases.

330

331 Clinical and prognosis significance of CD56+CTC

332 In order to correlate tumor burden and propensity to detect CTC in SCLC patients, we
333 compared the number of CD56+CTC according to the initial stage of the disease. Patients
334 with ES-SCLC show significantly higher number of CD56+CTC compared with patient
335 diagnosed with LS-SCLC (respective median of 7.95 vs 2.00; p=0.014) (Fig. 3A). To gain
336 further insight into the specific clinical parameters associated with higher numbers of CTCs
337 detected, we looked at each descriptor of the TNM classification (Fig 3B). Even if we
338 observed a trend toward a higher count of CD56+CTC in patient with more advanced T, N or
339 M status, statistical significance was not reached. As of December 2021, a relapse or death
340 event occurred in all patients in our cohort after first line-treatment. The median PFS was 5.2
341 months in the overall cohort with 5.2 months and 5.3 months in the low CD56+CTC group
342 and high CD56+CTC group, respectively (HR=0.80 CI 95% [0.39-1.56]; p=0.5) (figure 3C,
343 left panel). Median overall survival was 8.1 months in the overall cohort and no statistically
344 significant difference was observed between the two groups: 10.16 months in the low
345 CD56+CTC group versus 8.7 months in the high CD56⁺CTC group (HR=0.92 CI 95% [0.43-
346 1.93]; p=0.8) (figure 3C, right panel). Importantly, at the time of analysis, no difference in
347 survival was observed between ES-SCLC and LS-SCLC in our cohort (Supplemental Fig.5).

348

349 Somatic evolution of CD56+CTC at progression after first-line treatment

350 In order to decipher the tumor biology of SCLC at relapse, we conducted CD56+CTC
351 isolation for patient 04 at clinical progression (costal metastasis after 3 cycles of carboplatin-
352 etoposide). CD56+CTC counts were higher at relapse compared to diagnosis: 42 cells/ml
353 versus 8 cells/ml respectively. However, WES showed that the mutation load decreased
354 almost two fold in CD56+CTC at relapse (Fig. 3D). Interestingly, most of the mutations
355 (1667/2497=66.7%) observed in relapsed CD56+CTC were also detected in CD56+CTC
356 isolated at diagnosis (Fig. 3E). Conducting functional analysis enrichment, we were able to

357 identify differentially altered pathways between diagnosis and relapse circulating CD56+
358 tumor clones (Fig. 3F). Notably, signaling pathways known to drive tumorigenesis in SCLC
359 and currently investigated in targeted therapy trials (DLL3-targeting molecules for the
360 NOTCH pathway or PI3KCA/AKT inhibitors for the MAPK pathway) were specifically
361 implicated in relapsed CD56+CTC (19,20). These results suggest that overcoming relapse
362 after first-line systemic treatment may require targeting these signaling pathways, as we
363 speculate this gives a selective advantage for resurgent SCLC clones.

364

365 **Discussion**

366 This prospective study demonstrates the feasibility of an EpCAM-independent and
367 immunofluorescence-based CTC isolation in SCLC and its application in clinical practice. We
368 confirmed that CD56+CTC display a neuroendocrine tumor lineage and conserve tumorigenic
369 properties *in vivo* and *in vitro*. Coherently, whole-exome sequencing validated that
370 CD56+CTC show typical genomic alterations and classical altered pathways commonly found
371 in SCLC (e.g. TP53 mutation, RB1 loss) but they are also characterized by distinct mutational
372 patterns. We prospectively observed that ES-SCLC display a higher CD56+CTC count at
373 diagnosis compared to LS-SCLC. Finally, we show that detection of CD56+CTC at
374 progression after first-line treatment uncover new oncogenic pathways implicated in relapse
375 circulating tumor cells.

376 In line with previous results in non-small cell lung cancer, EpCAM-independent detection of
377 CTC show a high sensitivity (21). Indeed, median number of CTCs at baseline using
378 CellSearch® approach in a large SCLC cohort was 14 CTC/7.5ml of blood (14), compared to
379 28 CTC/7.5ml of blood in our cohort. Interestingly, in a recent cohort restricted to ES-SCLC,
380 the median number of CTC at diagnosis using CellSearch® was 30 CTC/7.5 ml of blood (22),
381 whereas it reaches 225 CTC/7.5 ml of blood in the ES-SCLC patients in our cohort. As EMT
382 is expected to be a more potent phenomenon when metastatic spread occurs, we speculate that
383 our EpCAM-independent method allow us to capture CTCs from SCLC that would remain
384 undetected using CellSearch® approach, especially in late-stage SCLC. Supporting this
385 hypothesis, similar observations were made in a large cohort of 108 SCLC patients where
386 CellSearch® failed to detect CTCs for 22 patients whereas immunofluorescence-based
387 approach succeeded (14). Moreover, intra- and inter-patient heterogeneity was observed for
388 EMT markers in both CTCs and circulating tumor microemboli in lung cancer (23) and could
389 partially explain these discrepancies.

390 To our knowledge, this study is the first to report genomic features of EpCAM-independent
391 CTC in SCLC. Beyond the confirmation of typical genomic alteration of SCLC in
392 CD56+CTC, we show that the mutational load was high compared to paired tumor biopsies or
393 published data on CTC of SCLC. This suggests that our EpCAM-independent method allows
394 us to capture more exhaustively CTC heterogeneity and altered signaling pathways. To
395 support this hypothesis we report a set of 75 hub genes altered in CD56+CTC, comprising 23
396 core genes shared with public SCLC genomic databases. Unique CTC genomic signatures
397 have been described in others solid malignancies (24,25), highlighting cell populations with
398 different functional or metastatic potential. In the context of SCLC, larger genomic studies
399 considering single-cell sequencing of EpCAM-independent CTC are needed to confirm the
400 new pathways we identified as altered in our dataset. Further longitudinal data from
401 sequencing of CTC at diagnosis and relapse are underway to establish firmly the relevant
402 common mechanisms that might drive resistance to therapy.

403 Prognostic value of CTC from SCLC has been extensively reported before. Indeed, Hou et al.
404 reported that more than 50 CTCs/7.5 ml of blood at diagnosis has a detrimental effect on PFS
405 and OS (6). Similarly, Su et al. and Carter et al. reported that copy-number-alteration (CNA)
406 analysis from single cell CTC could predict chemosensitivity status and PFS (7,10). In our
407 study, no difference of CD56+CTC numeration was observed based on the chemosensitivity
408 status of tumors and no association with prognosis was found based on the pre-specified cut-
409 off value of 7 CD56+CTC/ml. In line with this result, a recent work from Masseratakis et al.
410 et using an immunofluorescence CTC-isolation method did not show correlation between
411 CD56+CTC and clinical outcomes (14). Altogether, we hypothesized that CD56+CTC might
412 not correlate with the invasive potential or the aggressiveness of the primitive tumor and/or
413 might not dictate tumor sensitivity to systemic therapy. One caveat to this hypothesis is the
414 absence of an impact on survival of the stage of the disease in our cohort. Some confounding

415 factors and the relative small size of our cohort might have limited the power of the survival
416 analysis. A better understanding of the biology of EpCAM-negative CTC and of the processes
417 of EMT in SCLC is needed to definitely address this question.

418 Our study has several limitations. The cohort is relatively small and patients were recruited in
419 a single institution. A direct comparison of EpCAM-independent isolation method and
420 CellSearch® could not be performed as this technology is not available in our institution. We
421 also acknowledge that using CD56 as positive CTC selection marker might preferentially
422 capture CTC retaining neuroendocrine phenotype. However, it is unclear today if EMT
423 impacts neuroendocrine state of CTC. Masseratakis et al, confirmed the favorable
424 comparison of an immunofluorescence-based CTC isolation from SCLC (using CD56 and/or
425 TTF1) compared to the CellSearch® technology (14). However, no study has explored to date
426 the potential co-expression between EpCAM and CD56 markers on CTC from SCLC. Of
427 note, as combination of anti PD-L1 with chemotherapy was not at a standard of care during
428 the larger inclusion period of the study, we couldn't assess the relevance of CD56+CTC upon
429 immunotherapy. However, as EMT has been associated with inflammatory tumor
430 microenvironment and elevation of multiple targetable immune checkpoint molecules in lung
431 cancer (26), exploring the relation between CD56+CTC and EMT in the context of the new
432 immunotherapeutic strategies in SCLC would be an important avenue to explore.

433

434 **Conclusion**

435 Isolation of CD56+CTC using an immunofluorescence-based EpCAM-independent method at
436 diagnosis is feasible in SCLC and might capture more efficiently tumor genomic
437 heterogeneity. CD56+CTC are characterized by a high mutation load and a distinct mutational
438 signature from paired tumor biopsies. Above classical pathways altered in SCLC, we identify
439 new biological processes specifically affected in CD56+CTC. High numeration of
440 CD56+CTC is associated with ES-SCLC. Finally, detection of CD56+CTC at progression
441 after first-line treatment might help to understand somatic evolution of SCLC and elaborate
442 strategies overcoming therapeutic resistance.

443

444 **Bibliography**

- 445 1. Torre LA, Siegel RL, Jemal A. Lung Cancer Statistics. *Adv Exp Med Biol.* 2016;893:1–
446 19.
- 447 2. van Meerbeeck JP, Fennell DA, De Ruysscher DKM. Small-cell lung cancer. *Lancet*
448 *Lond Engl.* 2011;378:1741–55.
- 449 3. Horn L, Mansfield AS, Szczęsna A, Havel L, Krzakowski M, Hochmair MJ, et al. First-
450 Line Atezolizumab plus Chemotherapy in Extensive-Stage Small-Cell Lung Cancer. *N*
451 *Engl J Med.* 2018;379:2220–9.
- 452 4. Paz-Ares L, Dvorkin M, Chen Y, Reinmuth N, Hotta K, Trukhin D, et al. Durvalumab
453 plus platinum-etoposide versus platinum-etoposide in first-line treatment of extensive-
454 stage small-cell lung cancer (CASPIAN): a randomised, controlled, open-label, phase 3
455 trial. *Lancet Lond Engl.* 2019;394:1929–39.
- 456 5. Faivre-Finn C, Snee M, Ashcroft L, Appel W, Barlesi F, Bhatnagar A, et al. Concurrent
457 once-daily versus twice-daily chemoradiotherapy in patients with limited-stage small-
458 cell lung cancer (CONVERT): an open-label, phase 3, randomised, superiority trial.
459 *Lancet Oncol.* 2017;18:1116–25.
- 460 6. Hou J-M, Krebs MG, Lancashire L, Sloane R, Backen A, Swain RK, et al. Clinical
461 significance and molecular characteristics of circulating tumor cells and circulating
462 tumor microemboli in patients with small-cell lung cancer. *J Clin Oncol Off J Am Soc*
463 *Clin Oncol.* 2012;30:525–32.
- 464 7. Su Z, Wang Z, Ni X, Duan J, Gao Y, Zhuo M, et al. Inferring the Evolution and
465 Progression of Small-Cell Lung Cancer by Single-Cell Sequencing of Circulating Tumor
466 Cells. *Clin Cancer Res Off J Am Assoc Cancer Res.* 2019;25:5049–60.
- 467 8. Tay RY, Fernández-Gutiérrez F, Foy V, Burns K, Pierce J, Morris K, et al. Prognostic
468 value of circulating tumour cells in limited-stage small-cell lung cancer: analysis of the
469 concurrent once-daily versus twice-daily radiotherapy (CONVERT) randomised
470 controlled trial. *Ann Oncol Off J Eur Soc Med Oncol.* 2019;30:1114–20.
- 471 9. Hodgkinson CL, Morrow CJ, Li Y, Metcalf RL, Rothwell DG, Trapani F, et al. Tumorigenicity and genetic profiling of circulating tumor cells in small-cell lung cancer.
472 *Nat Med.* 2014;20:897–903.
- 474 10. Carter L, Rothwell DG, Mesquita B, Smowton C, Leong HS, Fernandez-Gutierrez F, et
475 al. Molecular analysis of circulating tumor cells identifies distinct copy-number profiles
476 in patients with chemosensitive and chemorefractory small-cell lung cancer. *Nat Med.*
477 2017;23:114–9.
- 478 11. Polioudaki H, Agelaki S, Chiotaki R, Politaki E, Mavroudis D, Matikas A, et al. Variable expression levels of keratin and vimentin reveal differential EMT status of
479 circulating tumor cells and correlation with clinical characteristics and outcome of
480 patients with metastatic breast cancer. *BMC Cancer.* 2015;15:399.

- 482 12. Krawczyk N, Meier-Stiegen F, Banys M, Neubauer H, Ruckhaeberle E, Fehm T.
483 Expression of stem cell and epithelial-mesenchymal transition markers in circulating
484 tumor cells of breast cancer patients. BioMed Res Int. 2014;2014:415721.
- 485 13. Hanssen A, Loges S, Pantel K, Wikman H. Detection of Circulating Tumor Cells in
486 Non-Small Cell Lung Cancer. Front Oncol. 2015;5:207.
- 487 14. Messaritakis I, Stoltidis D, Kotsakis A, Dermitzaki E-K, Koinis F, Lagoudaki E, et al.
488 TTF-1- and/or CD56-positive Circulating Tumor Cells in patients with small cell lung
489 cancer (SCLC). Sci Rep. 2017;7:45351.
- 490 15. Nicholson AG, Chansky K, Crowley J, Beyruti R, Kubota K, Turrisi A, et al. The
491 International Association for the Study of Lung Cancer Lung Cancer Staging Project:
492 Proposals for the Revision of the Clinical and Pathologic Staging of Small Cell Lung
493 Cancer in the Forthcoming Eighth Edition of the TNM Classification for Lung Cancer. J
494 Thorac Oncol. 2016;11:300–11.
- 495 16. Dual IRE1 RNase functions dictate glioblastoma development. EMBO Mol Med. John
496 Wiley & Sons, Ltd; 2018;10:e7929.
- 497 17. Blokzijl F, Janssen R, van Boxtel R, Cuppen E. MutationalPatterns: comprehensive
498 genome-wide analysis of mutational processes. Genome Med. 2018;10:33.
- 499 18. George J, Lim JS, Jang SJ, Cun Y, Ozretić L, Kong G, et al. Comprehensive genomic
500 profiles of small cell lung cancer. Nature. 2015;524:47–53.
- 501 19. Jin Y, Chen Y, Tang H, Hu X, Hubert SM, Li Q, et al. Activation of PI3K/AKT Pathway
502 Is a Potential Mechanism of Treatment Resistance in Small Cell Lung Cancer. Clin
503 Cancer Res. 2022;28:526–39.
- 504 20. Giffin MJ, Cooke K, Lobenhofer EK, Estrada J, Zhan J, Deegen P, et al. AMG 757, a
505 Half-Life Extended, DLL3-Targeted Bispecific T-Cell Engager, Shows High Potency
506 and Sensitivity in Preclinical Models of Small-Cell Lung Cancer. Clin Cancer Res Off J
507 Am Assoc Cancer Res. 2021;27:1526–37.
- 508 21. Hofman V, Ilie MI, Long E, Selva E, Bonnetaud C, Molina T, et al. Detection of
509 circulating tumor cells as a prognostic factor in patients undergoing radical surgery for
510 non-small-cell lung carcinoma: comparison of the efficacy of the CellSearch AssayTM
511 and the isolation by size of epithelial tumor cell method. Int J Cancer J Int Cancer.
512 2011;129:1651–60.
- 513 22. Cheng Y, Liu X-Q, Fan Y, Liu Y-P, Liu Y, Liu Y, et al. Circulating tumor cell
514 counts/change for outcome prediction in patients with extensive-stage small-cell lung
515 cancer. Future Oncol Lond Engl. 2016;12:789–99.
- 516 23. Hou J-M, Krebs M, Ward T, Sloane R, Priest L, Hughes A, et al. Circulating tumor cells
517 as a window on metastasis biology in lung cancer. Am J Pathol. 2011;178:989–96.
- 518 24. Kanwar N, Hu P, Bedard P, Clemons M, McCready D, Done SJ. Identification of
519 genomic signatures in circulating tumor cells from breast cancer. Int J Cancer.
520 2015;137:332–44.

- 521 25. Heitzer E, Auer M, Gasch C, Pichler M, Ulz P, Hoffmann EM, et al. Complex tumor
522 genomes inferred from single circulating tumor cells by array-CGH and next-generation
523 sequencing. *Cancer Res.* 2013;73:2965–75.
- 524 26. Lou Y, Diao L, Cuentas ERP, Denning WL, Chen L, Fan YH, et al. Epithelial-
525 Mesenchymal Transition Is Associated with a Distinct Tumor Microenvironment
526 Including Elevation of Inflammatory Signals and Multiple Immune Checkpoints in Lung
527 Adenocarcinoma. *Clin Cancer Res Off J Am Assoc Cancer Res.* 2016;22:3630–42.

528

529

530 **Figure and tables legends:**

531

532 **Figure 1. Isolation of CD56+CTCs and generation of pre-clinical models.** **A.** Schematic
533 workflow of the CTC-CPC study. **B.** Isolation procedure of CD56+CTC from whole blood
534 sample (left panel); Representative result of flow cytometry cell sorting (right panel). **C.**
535 Circulating tumor cells-derived xenograft (CDX) obtained from isolated CD56+CTC. **D.** IHC
536 phenotype of *in vivo* models obtained from isolated CD56+CTC (upper panel); *Ex vivo* cell
537 lines obtained from isolated CD56+CTC (lower panel). **E.** Heatmap and hierarchical
538 clustering based on the expression data of the four (established) key transcription regulators
539 that are (commonly) used to identify the SCLC molecular subtype. Samples are derived from
540 50 SCLC cell lines, from CCLE with known molecular subtypes and from one patient of
541 unknown SCLC subtype (CEM 18-03). For every gene, the color scale indicates its relative
542 expression, from blue (low) to red (high).

543

544 **Figure 2. Genomic characterization of CD56+CTC.** **A.** Heatmap of genomic alterations of
545 SCLC candidate genes (CTC samples of 4 patients). Mutation rates are displayed in the top
546 panel. **B.** Somatic copy number alterations in CD56+CTC (amplifications in red and deletions
547 in blue); lower panel shows copy number alteration in published SCLC genomic studies. **C.**
548 Venn diagrams represent non synonymous mutations (SNPs & InDels) in biopsies and
549 CD56+CTCs. **D.** Mutation spectrum plot illustrates the relative contribution of the 6 base
550 substitution types to the point mutation spectrum for each patient sample. Bars show the mean
551 relative contribution of each mutation type over all patient samples per sample type (biopsy
552 and CD56+CTC) and error bars indicate the standard deviation. **E.** Derived genomic signature
553 comprised of 75 genes for the CD56+CTC at the time of diagnosis. **F.** Analysis of the
554 Reactome pathway of the 75 genes CD56+CTC genomic signature (ranked according p-
555 value).

556

557 **Figure 3. Clinical significance of CD56+CTC at diagnosis and somatic evolution of CTC**
558 **at relapse.** **A.** Diagnosis numeration of CD56+CTC according to SCLC staging (*: p<0.05; #
559 : two values outside the limits of the graph). **B.** Numeration of CD56+CTC according to the
560 8th TNM IASCL classification (ns : non-significant) **C.** Kaplan-Meier curve of progression-
561 free-survival (left panel) or overall survival (right panel) according to the numeration of
562 CD56+CTC with a pre-specified cut-off value of 7 CTC/ml. **D.** Mutational load of all samples
563 from patient 04. **R.** Venn diagrams representing non synonymous mutations (SNPs & InDels)
564 in CTCs at diagnosis and after relapse (right) for patient 04. **F.** Analysis of the REACTOME
565 pathways of the common non synonymous genes (1667) at diagnosis and after relapse.

566

567 **Table 1. Genomic analysis of tumor biopsies and CD56+CTC.**

568

569 **Table 2. Cohort demographics.**

570

571 **Acknowledgement:**

572 We'd like to thank, la Region Bretagne, La Ligue Contre le Cancer (Grand Ouest),
573 l'Association pour la Recherche sur le Cancer (ARC) and Roche® company for their financial
574 supports to the CTC-CPC study. This work was also supported by ANR through the Labcom
575 Oncotrial projet 2014–2019 (Université de Rennes 1 – UAR Biosit – BIOTRIAL, Rennes,
576 France), notably through grants to UJ, RP & TG, and by the “Région Bretagne” as part of a
577 collaborative project with Biotrial supported by “Biotech Santé Bretagne”. We thank the cell
578 sorting facility (Cytometry, UAR Biosit, Rennes, France), the histopathology facility (H2P2,
579 UAR Biosit, Rennes, France) for their technical expertise and the animal facility the animal
580 facility (Arche, UAR Biosit, Rennes, France) for animal husbandry and care. We thank the
581 DRCI department of the CHU Rennes for administrative support.
582

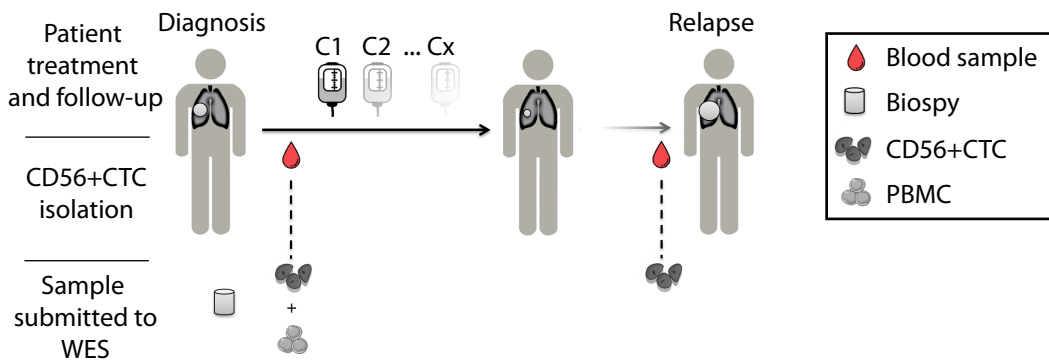
583 **Data and code availability**

584 Whole-exome sequencing data have been deposited in the ArrayExpress database at EMBL-
585 EBI (www.ebi.ac.uk/arrayexpress) under accession number E-MTAB-10766 at eh following
586 address : <https://www.ebi.ac.uk/biostudies/arrayexpress/studies/E-MTAB-10766?key=362b5948-a5e9-4026-bbef-943c1703cbdf>. Additional supplementary files from
587 the computational integrative workflow, R scripts and command line code implemented to
588 reproduce the analysis are available on the Zenodo open data repository
589

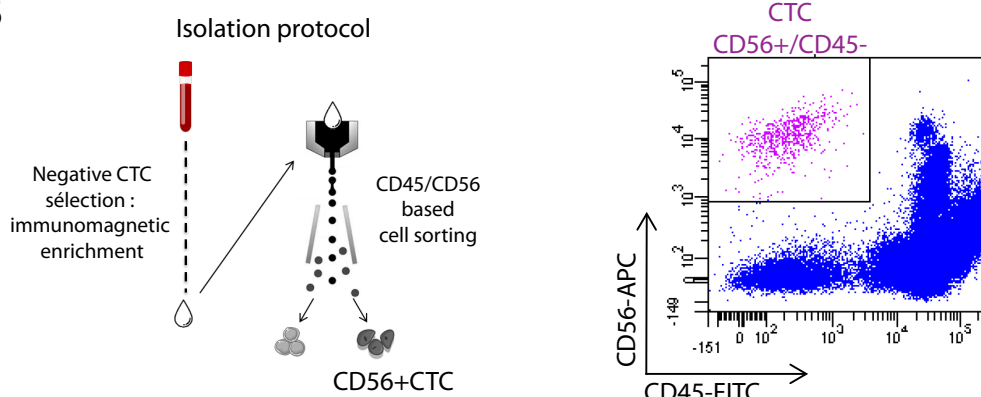
Figure 1

bioRxiv preprint doi: <https://doi.org/10.1101/2022.04.30.487775>; this version posted March 8, 2023. The copyright holder for this preprint (which was not certified by peer review) is the author/funder. All rights reserved. No reuse allowed without permission.

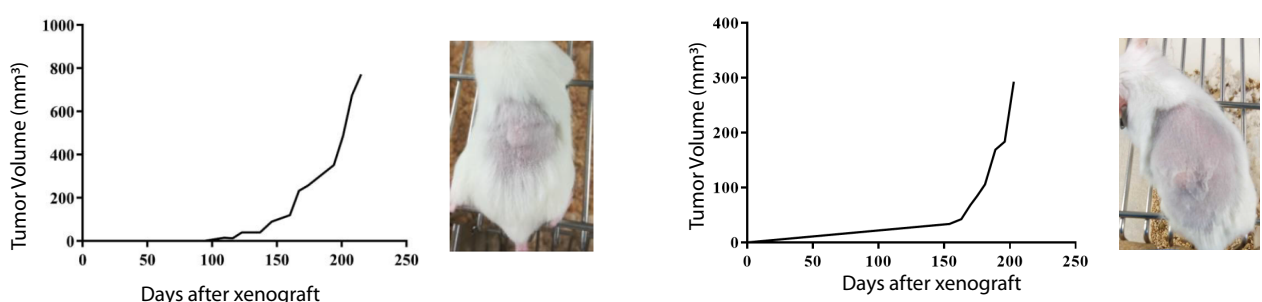
A



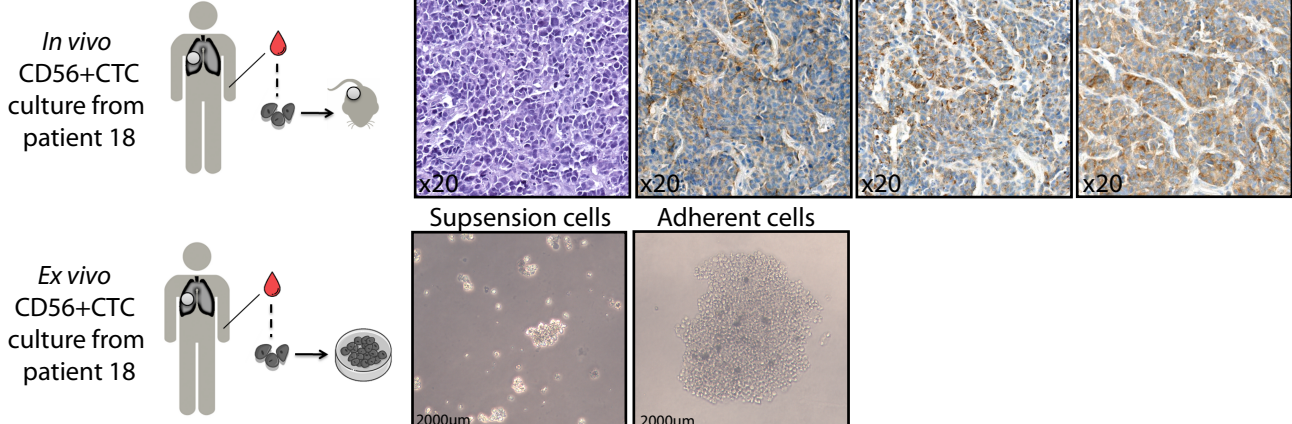
B



C



D



E

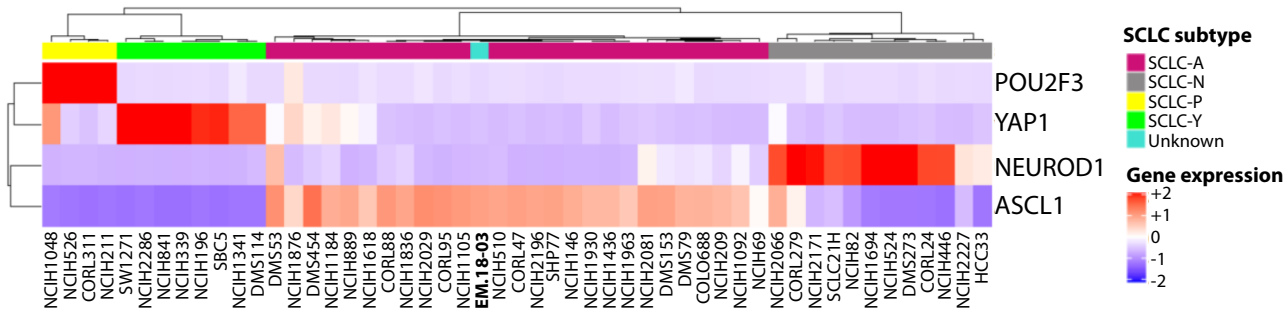


Figure 2

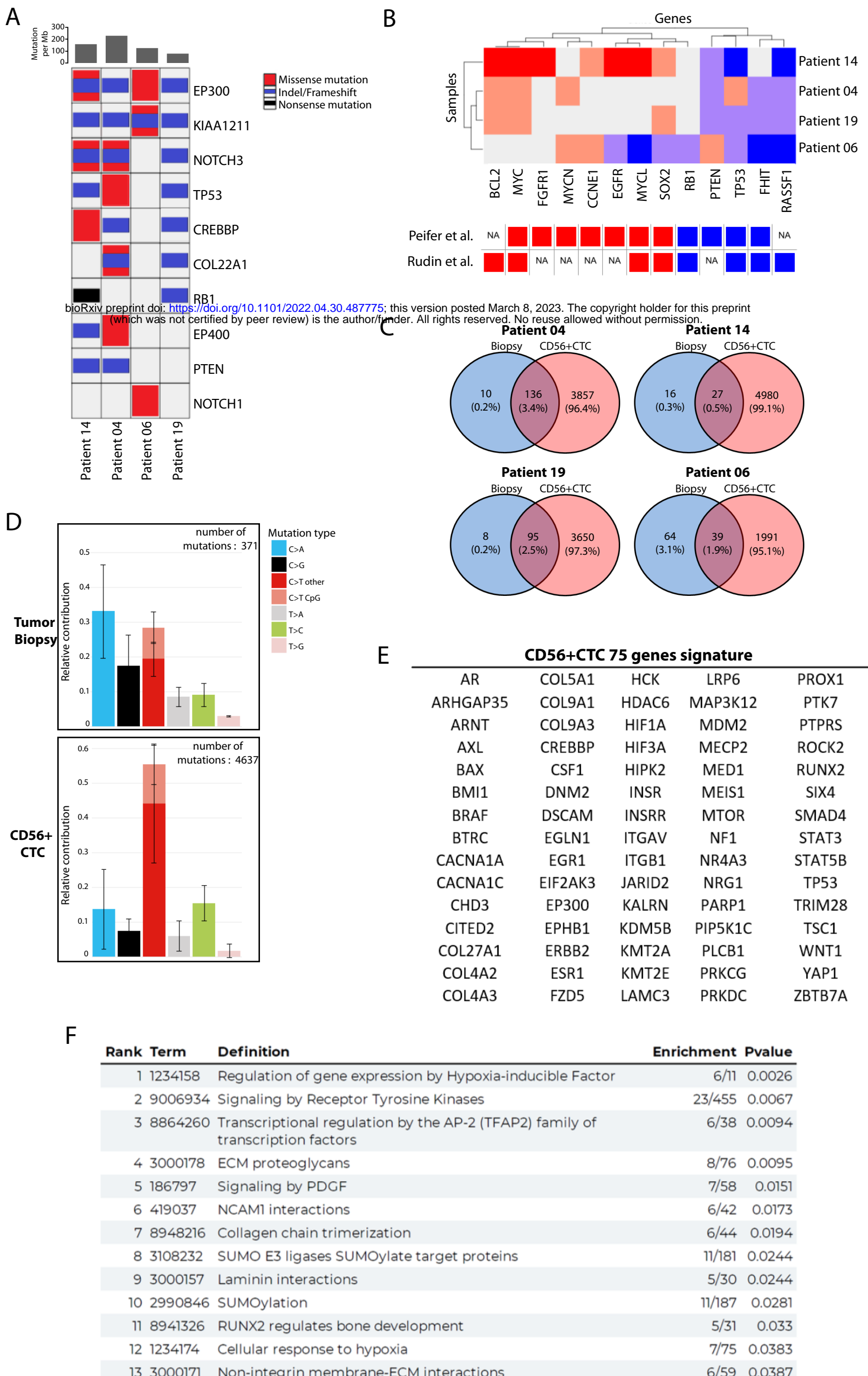
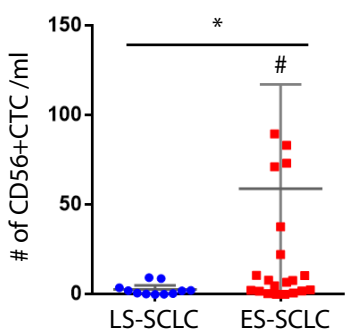


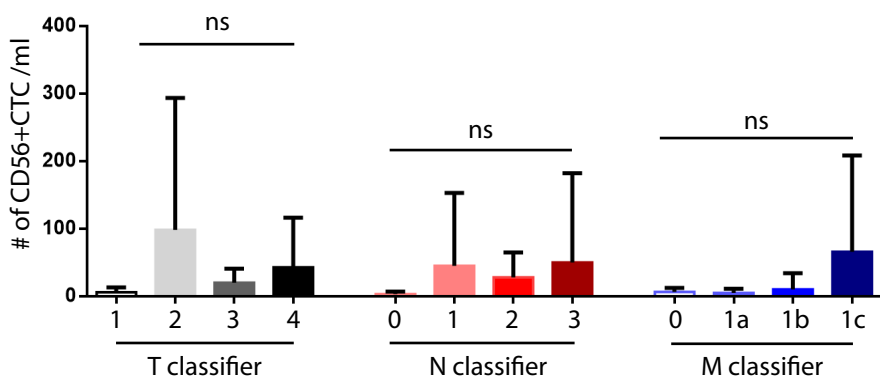
Figure 3

bioRxiv preprint doi: <https://doi.org/10.1101/2022.04.30.487775>; this version posted March 8, 2023. The copyright holder for this preprint (which was not certified by peer review) is the author/funder. All rights reserved. No reuse allowed without permission.

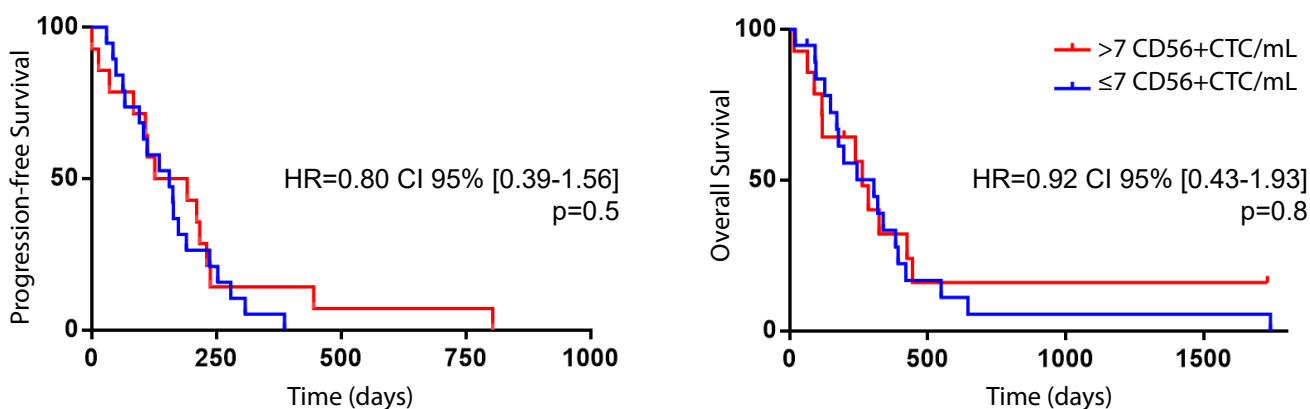
A



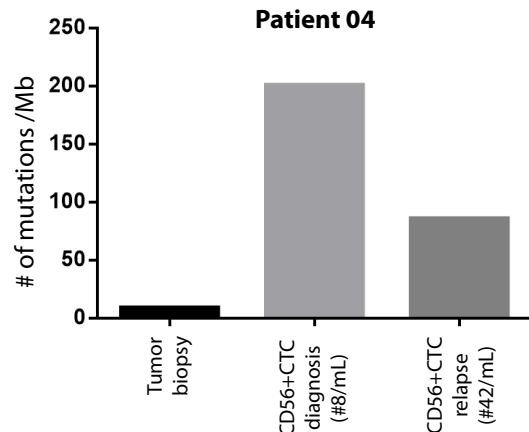
B



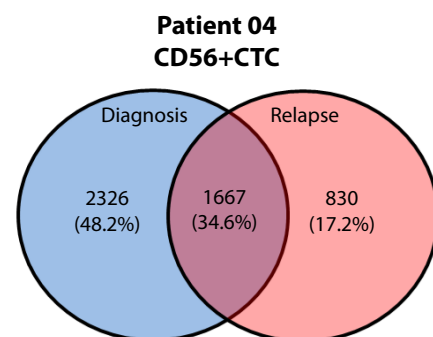
C



D



E



F

Rank	Term	Definition	Enrichment	P value
1	452723	Transcriptional regulation of pluripotent stem cells	6/31	0.0017
2	212676	Dopamine Neurotransmitter Release Cycle	5/23	0.0039
3	6794362	Protein-protein interactions at synapses	10/88	0.0055
4	210747	Regulation of gene expression in early pancreatic precursor cells	3/8	0.0082
5	8874211	CREB3 factors activate genes	3/9	0.0113
6	8856828	Clathrin-mediated endocytosis	13/145	0.0114
7	879518	Transport of organic anions	3/12	0.0146
8	199418	Negative regulation of the PI3K/AKT network	10/110	0.0161
9	9012852	Signaling by NOTCH3	6/49	0.0161
10	1257604	PIP3 activates AKT signaling	18/264	0.0194
11	9013507	NOTCH3 Activation and Transmission of Signal to the Nucleus	4/25	0.0211
12	9006925	Intracellular signaling by second messengers	20/303	0.0229
13	5675221	Negative regulation of MAPK pathway	5/40	0.0279
14	6811558	PIP5P, PP2A and IER3 Regulate PI3K/AKT Signaling	9/103	0.03